Cell

EXTENDED EXPERIMENTAL PROCEDURES

Materials

Egg L-α-phosphatidylcholine (EPC), brain sphingomyelin (BSM), L-α-phosphatidylinositol-4,5-bisphosphate (PIP_2), di-stearoyl phosphatidyl ethanolamine-PEG(2000)-Biotin (DSPE-PEG2000-Biotin), cholesterol and 1-stearoyl-2-hydroxy-*sn*-glycero-3-phosphocholine (Lyso PC) were purchased from Avanti Polar Lipids, Alabaster, Alabama, USA. BodipyTMR-PIP_2 ($RedPIP_2$) was purchased from Echelon Bioscience, Salt Lake City, Utah, USA, and Guanosine Triphosphate (GTP) from Roche Applied Science, Indianapolis, Indiana, USA. Five lipid preparations were used (molar percentage): 80% EPC + 19%PIP_2 + 1%$RedPIP_2$; 70% EPC + 10% BSM + 19%PIP_2 + 1%$RedPIP_2$ supplemented with 40% cholesterol; 80% EPC + 19%PIP_2 + 1%$RedPIP_2$ supplemented with 50% cholesterol; 80% BSM + 19%PIP_2 + 1%$RedPIP_2$ supplemented with 50% cholesterol and 50% EPC + 30% Lyso PC + 19% PIP_2 + 1%$RedPIP_2$. These five mixtures also contained 0.03% DSPE-PEG2000-Biotin.

Protein Purification

Recombinant human dynamin 1 was purified from Sf9 cells infected with recombinant baculovirus using the BD baculogold expressing system (BD Biosciences, Franklin Lakes, NJ USA). Dynamin was purified from cell lysate with the GST-tagged SH3 domain of rat Amphiphysin 1 as an affinity ligand as previously described (Stowell et al., 1999). Briefly, cells from twenty 150cm^2 flasks were resuspended in 20 ml of Buffer A (20 mM HEPES pH 7.4, 100 mM NaCl, 1 mM EGTA, 1 mM DTT, 1% Triton X-100) supplemented with the protease inhibitor cocktail (cOmplete ULTRA Tablets, Roche Applied Science, Indianapolis, Indiana, USA) and homogenized with a 60 ml dounce. The lysate was centrifuged at 40krpm on a Ti70 rotor (Beckman-Coulter, Brea, CA), and the supernatant was incubated for 2 hr with glutathione beads to which 3-5 mg of purified GST-SH3 domain of rat Amphiphysin 1 were attached. Next, the beads were batch-washed with 150 ml of Buffer A without Triton X-100. Elution was done with high salt (20 mM HEPES, pH 7.4, 1.2 M NaCl, 1 mM $MgCl_2$). Unlabeled dynamin was dialyzed against storage buffer (20 mM HEPES, pH 7.4, 100 mM NaCl, 1 mM $MgCl_2$), concentrated using Amicon (50kDa CO), aliquoted, flash-frozen in liquid N_2 and stored at −80°C.

To fluorescently label dynamin, we dialyzed dynamin against PBS 50% glycerol. The labeling reaction was conducted using standard procedures (Alexa-488 protein labeling kit from Invitrogen, cat# A-10235). In some case, dynamin 1 was labeled with Alexa Fluor 488 C5 maleimide (Molecular Probes, Life Technologies, Paisley, UK). To attach streptavidin-coated microbeads to dynamin polymers, dynamin was conjugated to DSB-X Biotin C2-iodoacetamide (Molecular Probes, Life Technologies, Paisley, UK). Labeled dynamins were dialysed against storage buffer, aliquoted and kept at −80°C.

Nanotube Pulling from GUV

Lipid mix (0.5 mg/ml) was deposited on indium-tin oxide coated glass slides and dried 1h at 55°C to remove all solvents. GUVs were electroformed (1V, 10Hz) (Angelova et al., 1992; Stowell et al., 1999) for 1h at 55°C in a 200 mM sucrose solution then transferred in an observation chamber pretreated with Casein solution (2 mg/ml). GUVs were aspirated in a micropipette controlled with a motorized micromanipulator (MP-225, Sutter Instrument, Novato, California, USA) and a custom-made hydraulic system to control aspiration pressure ΔP and to set the tension: $\sigma = 1/2(R_{pipette}\Delta P/(1 - R_{pipette}/R_{GUV}))$ where $R_{pipette}$ and R_{GUV} are the radii of the pipette and the GUV respectively (Evans and Rawicz, 1990). A membrane nanotube was formed by pulling away a micropipette aspirated GUV whose membrane was attached to a streptavidin-coated bead (3.05 μm diameter, Spherotec, Lake Forest, Illinois, USA) hold in a fixed optical trap. The custom-made optical trap was made by focusing an ytterbium fiber laser (IPG laser, Burbach, Germany) through a 100X 1.3 NA oil immersion objective (Nikon, Tokyo, Japan). The force F exerted on the bead was calculated from the Hooke's law: F = k*Δx where k is the stiffness of the trap (k = 360pN.μm^{-1}.W^{-1}) calibrated by viscous drag method (Neuman and Block, 2004) and Δx the displacement of the bead from its equilibrium position in the optical trap. Video-rate movies and displacement measurements were done via a C-MOS Camera (Pixelink, Ottawa, Canada) with a user-made video recorder and bead tracking software under Matlab.

Dynamin and GTP were injected close to the nanotube with a second micropipette of typical 10 micron radius controlled with a hydraulic micromanipulator (Narishige, Tokyo, Japan). Nanotubes were observed simultaneously by bright field imaging and by dual-color confocal microscopy (λ1 = 488 nm and λ2 = 543 nm) on a Nikon eclipse Ti inverted microscope (Nikon, Tokyo, Japan). For fast 2-colors confocal experiments, a spinning disk (Intelligent Imaging Innovations, Denver, CO) and a two-channel simultaneous-imaging system (Dual-View, Photometrics, Tucson, AZ) were used instead of standard confocal microscopy (Eclipse C1 Confocal, Nikon, Tokyo, Japan).

Membrane Sheets and Dynamin Tubules Formation

To form membrane sheets, 22x40 mm glass coverslips were first cleaned by sonication (5 min) in 1% Decon 90, Modec, USA, in distilled water. After thorough washing and sonication (5 min) in distilled water to remove any trace of detergent, coverslips were finally washed with 100% ethanol prior to storage in ethanol. Coverslip were dried under a N_2 flux, and 1μl droplets of lipid solution (10 mg/ml in pure chloroform) were deposited and allowed to dry on the coverslip. Typically, two drops were deposited at different sites on a same coverslips. The use of pure chloroform was essential to allow lipid droplet drying in a way that was optimal for the subsequent formation of membrane sheets upon hydration. Coverslips were then dried again under vacuum (0.2 milli-torr) for at least one hour, and kept up to several days under vacuum.

Before use, coverslips were placed for 20–30 min in a wet incubator (37°C, 100% humidity) to allow partial hydration of the lipids. Next, a small chamber (approximately 15 μl volume) was built by placing the coverslip onto a glass slide, with the lipids facing the glass slide, using a double-sided Scotch (3M) tape as a spacer. The lipids were fully rehydrated by applying to the side of the chamber 15–20 μl of GTPase buffer (20 mM HEPES pH 7.4, 100 mM NaCl, 1 mM $MgCl_2$) containing 0.1 mg/ml casein (C7078, Sigma) (casein buffer) which were taken up into the chamber by capillarity. Lipid deposits then transformed into membrane sheets. Dynamin solution, typically 0.5-1 mg/ml was then added to the side of the chamber, and transferred into the chamber by capillarity. Membrane sheets were then deformed into dynamin-coated tubules visible by DIC (Morlot et al., 2010; Roux et al., 2006).

Torque Measurement by Viscous Drag

Streptavidin beads (1.35 μm diameter streptavidin-coated, polystyrene beads, Spherotec, Lake Forest, IL) were grafted onto biotinylated dynamin tubules formed from membrane sheets (Morlot et al., 2010; Roux et al., 2006) by adding them to the chamber after tubule growth. The beads rotate following GTP addition and resulting constriction of the dynamin coat (Morlot et al., 2010; Roux et al., 2006), experiencing a viscous torque $\Gamma_v = 14\pi\eta(R+r)^3\ \omega = \xi\omega$ (Happel and Brenner, 1983), where η is the viscosity of the surrounding fluid, *R* the radius of the bead, *r* the radius of the tubule and ω is the angular spinning velocity. Differential Interference Contrast (DIC) and computer-based live recording of the rotating beads with a GUPPY camera (Allied Vision Technologies, Stadtroda, Germany) allowed direct measure of the angular spinning velocity and estimation of the viscous torque from the formula above.

Stall Torque Measurement by Magnetic Field

To measure the stall torque Γ_S that arrests the constriction of the membrane tube, we use a magnetic bead, to which an external torque via a variable magnetic field. The observation chamber (Figure S2A) is placed on the stage of an Axiovert 100 microscope (Zeiss, Oberkochen, Germany) equipped with a differential interference contrast (DIC), a fluorescence lamp and a UI-2220SE charge-coupled-device (CCD camera - IDS, Obersulm, Germany). The magnetic field to manipulate the magnetic beads is generated by two homemade electromagnets (see Figure S2B). Both the electromagnets are controlled using a NI USB-6211 multifunction data acquisition card (National Instruments, Austin, Texas, USA) and a homemade power supply. Magnets are calibrated using a DC magnetometer (AlphaLab, West Salt Lake City, UT). The bead motion is recorded and tracked using user-developed procedure under MATLAB.

To calibrate the torque induced by the magnetic field, the bead is attached to a dynamin-lipid nanotube and oriented with a magnetic field parallel to the coverslip (position "1" in the schema shown in Figure S2C, top). When the magnets polarity is switched, the bead rotates around the nanotube to follow the magnetic field and goes from position "1" to position "2." According to Langevin's equation, the angular speed $\omega(\theta)$ of the bead is proportional to the magnetic torque $\Gamma(\theta)$

$$\varepsilon\omega(\theta) = \Gamma(\theta) + \mu(t) = \Gamma_{max}\ \sin(\theta) + \mu(t),$$

Where ε is the viscous drag of the bead, $\mu(t)$ is a thermal noise and Γ_{max} is the torque exerted when the magnetic moment of the bead is perpendicular to the field ($\theta = \pi/2$). As the thermal noise is negligible compared to the magnetic torque, the maximal angular speed $\omega(\theta = \pi/2) = \varepsilon\Gamma_{max}$, where $\varepsilon = 14\ \pi\ \eta(R+r)^3$ (see above [Happel and Brenner, 1983]). In our measurements η is the viscosity of the water (1 mPa·s), *R* is the radius of the bead (655nm) and *r* is the radius of the dynamin-coated tube (25 nm). For each bead Γ_{max} is evaluated for different magnetic fields (Figure S2C, bottom).

Alternatively, the torque is calibrated with respect to the applied magnetic field through the thermal fluctuations of the beads. According to the equipartition theorem, the mean square amplitude of angular fluctuations is:

$$\Delta\vartheta^2 = \frac{k_B T}{\kappa_\Gamma},$$

where k_B is the Boltzmann constant, *T* is the temperature and $\kappa_\Gamma = -\partial\Gamma/\partial\vartheta|_{\Gamma=0}$ is the curvature of the magnetic potential around its minimum. The magnetic dipole moment is evaluated for different magnetic field *B* to obtain the calibration curve $\Gamma(B,\theta)$.

Cell Transfection, Treatment, and Imaging

COS-7 cells were transfected using FuGENE-6 (Roche Applied Science, Indianapolis, IN) with dynamin 2 fused to Green Fluorescent Protein (GFP) (kindly provided by P. De Camilli; HHMI, Yale University) or mouse clathrin-light-chain fused to mCherry or GFP (kindly provided by C. Merrifield, Cambridge and by P. De Camilli, HHMI, Yale University). Cells were imaged 18 to 24 hr post transfection in Leibovitz medium (GIBCO, Life Technologies, Paisley, UK). While imaging, the medium was changed with a hypertonic solution of 0.25 M sucrose in Leibovitz medium. Cell membrane staining was achieved by incubating cells for 5′ at 37°C with deep red Cell Mask (Molecular Probes, Life Technologies, Paisley, UK) before imaging. Genome edited SK-MEL-2 cells expressing dynamin2-GFP and clathrin Light Chain-RFP were provided by D.G. Drubin (University of California Berkeley, USA).

Transferrin Labeling

Cells were starved in serum deprived DMEM-F12 medium for 30 min on ice, then incubated with 5 μg/ml Alexa-fluor 594 Transferrin (Invitrogen) in hypertonic medium (0.25 M sucrose Leibovitz medium) for 3′ at RT. Cells were washed with hypertonic buffer before imaging.

Image Analysis

Images were analyzed and processed with ImageJ. Kymographs were made with Multiple Kymograph plugin (J. Rietdorf; A. Seitz). Fits were made with the curve fitting toolbox in Matlab.

Membrane Shape Computation

In this section we first derive the equilibrium equation for the shape of the membrane from Canham-Helfrich Hamiltonian and express the shape computation as a boundary value problem suitable for solution with Matlab's bvp4c.

Canham-Helfrich Hamiltonian gives the energy of the membrane as a function of its shape:

$$E = \sigma \int dA + \frac{\kappa}{2} \int J^2 dA.$$

The first term is related to the energy cost of stretching the membrane and σ is the membrane tension which can be controlled in the experiment. The second term represents the energy cost of bending which is given by the integral of membrane curvature J over the surface. The bending modulus κ depends on the composition of the membrane.

Considering the axial symmetry of the experiment we will restrict ourselves to axisymmetric shapes. For an axisymmetric surface with an axial coordinate z, and angle φ around the z axis, and a radius $r(z)$, curvature can be expressed as:

$$J = \frac{r(z)r''(z) - r'(z)^2 - 1}{r(z)\left(1 + r'(z)^2\right)^{3/2}}.$$

Writing the area element in the same coordinates $dA = r(z)\sqrt{r'(z)^2 + 1}dzd\varphi$, the integral in the angle φ can be directly performed and the energy can be cast in the following form:

$$E = \int \left(\sigma + \frac{\kappa}{2}J^2\right) r(z)\sqrt{r'(z)^2 + 1}dzd\varphi = 2\pi \int \left(\sigma + \frac{\kappa}{2}J^2\right) r(z)\sqrt{r'(z)^2 + 1}dz.$$

It will be convenient for numerical solution of the equations to nondimensionalize the Hamiltonian using the bare membrane radius $R_m = \sqrt{\kappa/2\sigma}$ to rescale all lengths, and $\pi\kappa$ to rescale the energy:

$$e = \int \left(1 + j^2\right)\rho(\theta)\sqrt{\dot{\rho}(\theta)^2 + 1}d\theta = \int \ell(\rho(\theta), \dot{\rho}(\theta), \ddot{\rho}(\theta))d\theta,$$

where

$$j = \frac{\rho(\theta)\ddot{\rho}(\theta) - \dot{\rho}(\theta) - 1}{\rho(\theta)\left(1 + \dot{\rho}(\theta)^2\right)^{3/2}}, \rho(\theta) = \frac{r(z)}{R_m}, \theta = \frac{z}{R_m}, e = \frac{E}{\pi\kappa}, \ell = \left(1 + j^2\right)\rho(\theta)\sqrt{\dot{\rho}(\theta)^2 + 1}$$

are all adimensional quantities and the dot represents differentiation with respect to θ. At equilibrium, membrane shape minimizes the energy. Thus, the equilibrium shape is given by the solution of Euler-Lagrange equation

$$\frac{d\ell}{d\theta} = \frac{d}{d\theta}\frac{\partial \ell}{\partial \dot{\rho}} - \frac{d^2}{d\theta^2}\frac{\partial \ell}{\partial \ddot{\rho}},$$

which is the nonlinear fourth order differential equation:

$$\left(-1 - 6\dot{\rho}^2 - 10\dot{\rho}^3 - 9\dot{\rho}^4 - 10\dot{\rho}^5 - 4\dot{\rho}^6 + \rho\ddot{\rho}\left(3 + 30\dot{\rho} - 9\dot{\rho}^2 - 40\dot{\rho}^3 - 12\dot{\rho}^4\right) + \rho^2\left(1 + \dot{\rho}^2\right)\left(1 + \dot{\rho}^4 + \dot{\rho}^6 + 3\ddot{\rho}^2 + \dot{\rho}^2\left(3 - 12\ddot{\rho}^2\right)\right.\right.$$
$$\left.\left. + 4\dot{\rho}\dddot{\rho} + 4\dot{\rho}^3\dddot{\rho}\right) + \dot{\rho}^3\left(5\left(-1 + 6\dot{\rho}^2\right)\ddot{\rho}^3 - \left(1 + \dot{\rho}^2\right)\ddot{\rho}\left(1 + 2\dot{\rho}^2 + \dot{\rho}^4 + 20\dot{\rho}\dddot{\rho}\right) + 2\left(1 + \dot{\rho}^2\right)^2\ddot{\rho}\right)\right) = 0$$

This equation was solved in the domain $\theta\varepsilon[0, 10]$, with two different sets of boundary conditions. For the junction between the tube and the dynamin-coated tube, it was required that

$$\rho(0) = 1, \dot{\rho}(0) = 0$$

$$\rho(10) = r_d, \dot{\rho}(10) = 0$$

with $r_d = R_d/R_m$ the adimensional dynamin radius, which was varied to compute the energy at different levels of constriction.

For the neck joining the vesicle or bead to the dynamin-coated tube, boundary conditions were

$$\rho(0) = 20, \rho(0)\ddot{\rho}(0) - \dot{\rho}(0) - 1 = 0$$

$$\rho(10) = r_d, \dot{\rho}(10) = 0.$$

The first condition ensures membrane joins the flat wall that mimics the vesicle at $\theta = 0$ with vanishing curvature. See the following parts of the Extended Experimental Procedures for more details on the rationale for these boundary conditions.

Boundary conditions for the vesicle geometry do not directly produce a solution with Matlab's bvp4c boundary value problem solver. A technique known as *continuation* was used to find the desired solution. The solution for a less *stringent* boundary condition (i.e., giving a less bent membrane) with $\rho(0) = 7, \rho(10) = 1$ was first computed and used as initial guess for a subsequent iteration with a slightly greater value of $\rho(0)$. This process was then repeated until the desired $\rho(0) = 20$ condition was met. Finally, the same process was used to decrease $\rho(10)$ from 1 to the desired value r_d.

Once membrane shapes were computed, we calculated the corresponding energy by numerical integration of Canham-Helfrich Hamiltonian.

Theory for Reduced Fission Energy Barrier at the Dynamin-Membrane Edge

We model membrane fission as a one-step reaction thermally activated with a single energy barrier, biased by the GTP hydrolysis driven constriction force. The radius R_d, that is, the radius of the dynamin-coated membrane, constitutes the reaction coordinate. In this analogy, the radius R_d is a brownian degree of freedom that may overcome a fission energy barrier by thermal fluctuations. GTP hydrolysis by dynamin generates a constriction force which in our model would operate as a force on the R_d degree of freedom, tilting the energy landscape and decreasing the total energy barrier ΔE_{tot} to a smaller value ΔE_{res}, biasing the transition toward the fission state (see Figure 2A in main text).

The energy barrier originates from differences in elastic and surface energy of the membrane neck that joins the edge of the dynamin-coated part to the bare tube with radius R_d, set by tension and bending rigidity.

After constriction, the residual barrier can be overcome by thermal fluctuations of the constricted radius, at a rate

$$r = \tau^{-1} e^{-\Delta E_{res}/k_b T}$$

where τ is a molecular characteristic time of reaction, k_b is the Boltzmann constant, T the temperature. A constant rate of reaction yields an average fission time

$$\langle t_f \rangle = \tau e^{\Delta E_{res}/k_b T}$$

A process with just one constant rate of reaction r gives an exponential distribution of reaction times

$$\rho(t_f) = r e^{-r t_f}$$

and consequently a cumulative probability of reaction

$$F(t_f) = \int_0^{t_f} \rho(x) dx = 1 - e^{-r t_f}.$$

Our experiments both present an exponential distribution of fission times (data not shown) and the corresponding cumulative probability is well fit by $1 - e^{-r t_f}$ as shown in Figure 3B in the main text.

To compute the bending and surface energy of the membrane we numerically solved the nonlinear shape equation that arises from Canham-Helfrich Hamiltonian minimization (see above) for the neck joining a bare membrane tube with a dynamin-coated one (see Figure 1G in the main text). This implies boundary conditions where the radius matches the bare tube radius R_m on one side and R_d, the radius of the dynamin-coated part, on the other. In both ends, the derivative of the radius with respect to the axial coordinate must vanish to smoothly join either the bare or dynamin-coated tube. The equation was numerically solved using Matlab bvp4c boundary problem solver for different values of R_d and constant R_m. From the shape, we compute the bending and surface energy energy $E(\alpha)$ as a function of dimensionless parameter $\alpha = R_m / R_d$, as depicted in Figure 2B.

To estimate the energy barrier we assume dynamin polymerizes and constricts the dynamin-coated membrane very fast compared to fission times (Morlot et al., 2010) to a radius R_c of the order of 4-5nm in the presence of GTP (the actual R_c should depend on GTP concentration in our model as fission time decreases with increasing GTP concentration; we nevertheless disregard this dependence for the sake of simplicity by taking a fixed GTP concentration and defer the discussion on the effect of GTP concentration for a later section). The coated membrane tube is still connected to the bare membrane tube by a neck-like shape. In order for the membrane to break, it makes a transition from this configuration with $R_d = R_c$, to another with a constricted radius $R_d = R_i$ corresponding to a hemifission intermediate state with a radius R_i independent of tension and bending rigidity. A hemifission intermediate is a state where the internal monolayer of the membrane is fused while the outer monolayer keeps its integrity. Evidence for the existence of a hemifission state has already been reported in (Bashkirov et al., 2008). Kozlovsky and Kozlov have proven for a different but related geometry where a constricted neck also exists that once this hemifission intermediate is attained the transition to complete fission proceeds spontaneously, due to a negative free energy difference between hemifission and complete fission state (Kozlovsky

and Kozlov, 2003). We assume there is no barrier once the hemifission is attained and therefore the fission reaction quickly proceeds to fission.

Hence, the energy barrier is the difference between the energy of these two configurations

$$\Delta E_{res}^{tube} = E\left(\frac{R_m}{R_i}\right) - E\left(\frac{R_m}{R_c}\right) \equiv E_i^{tube} - E_c^{tube}.$$

Taking R_i of the order of 3-5nm and R_c in the range 4-5nm and for the R_m used in our experiment, the ratio α ranges from 1 to 10, which allows us to approximate $E(\alpha)$ by a straight line with slope $\alpha \simeq 1/4$ and get an analytical prediction of the barrier dependence with tension and bending modulus

$$E \simeq a2\pi\kappa(\alpha - 1) \Rightarrow \Delta E_{res}^{tube} \simeq 2\pi a\left(\frac{1}{R_i} - \frac{1}{R_c}\right) \frac{\kappa^{3/2}}{\sqrt{2\sigma}},$$

where we already substituted the value of the bare membrane radius $Rm = \sqrt{\kappa/2\sigma}$.The average fission time thus depends on membrane parameters as

$$\langle t_f \rangle = \tau e^{\frac{b\kappa^{3/2}}{k_b T\sqrt{\sigma}}}$$

giving for *log* $\langle t_f \rangle$ a dependence

$$log\langle t_f \rangle = \log \tau + \frac{b\kappa^{3/2}}{k_b T\sqrt{\sigma}},$$

which fits all the experimental data for different values of κ and σ as shown in Figure 3 in the main text.

Fission at GUV-Dynamin or Bead-Dynamin Edge

As explained in the main text, fission occurs preferentially at the boundary between the tube and the GUV or between the tube and the bead. To analyze these cases we solved the shape equation with a modified boundary condition at GUV/bead's end. Due to the difference in size between the tube and the bead or GUV we can approximate GUV/bead by an infinite flat membrane wall perpendicular to the tube. This can be mimicked in the numeric computations by requiring that membrane radius at the wall (GUV) is much bigger than R_d and that membrane joins smoothly to a flat membrane, i.e., with vanishing curvature. At dynamin's edge, membrane has a radius R_d and enters the dynamin domain with vanishing slope to smoothly match the dynamin-coated tube. The dynamin coating is assumed to progress until a distance $10R_m$ from the flat wall. This coincides with the end of the bare tube that would form in the absence of dynamin (Derényi et al., 2002) and we expect the dynamin polymer to grow approximately until that position. Varying R_d again we can compute the energy as a function of α. The energy of the GUV-dynamin edge has the same approximate shape as in the bare tube-dynamin case (see Figure 2B) and therefore the above discussion remains valid, giving a similar dependence with κ and σ for fission time. Furthermore, the residual energy barrier for the vesicle or bead edge for $\kappa = 16k_bT$, $R_i = 3nm$ and $R_c = 4.5nm$ ranges from 20 k_bT to 23 k_bT as a function of tension σ giving an expected fission time

$$\langle t_f \rangle = \tau e^{\frac{\Delta E_{res}^{ves}}{k_b T}},$$

which agrees with experimentally observed times. Using hydrodynamic arguments we can estimate $\tau \approx 10^{-9}$s giving in turn fission times in the range [1, 13]s depending on tension, in agreement with experimental fission times.

Higher Probability of Fission at GUV's End

Differences in energy barrier for fission at the GUV-dynamin and at the tube-dynamin neck translate in different rates of fission. Disregarding differences in the number of tube-dynamin versus GUV-dynamin edges in front of the exponential factors, the probabilities to find a break in the GUV or tube edge in an experiment would be proportional to the rates of fission. According to our model, rates are exponentially related and therefore:

$$\frac{P_{ves}}{P_{tube}} = \frac{e^{-\Delta E_{res}^{ves}/k_B T}}{e^{-\Delta E_{res}^{tube}/k_B T}} = e^{\left(\Delta E_{res}^{tube} - \Delta E_{res}^{ves}\right)/k_B T}$$

with ΔE_{res}^{tube} and ΔE_{res}^{ves} the barriers for fission at the tube or vesicle respectively. Using normalization $P_{ves} + P_{tube} = 1$ we find

$$P_{ves} = \frac{1}{1 + e^{\left(\Delta E_{res}^{ves} - \Delta E_{res}^{tube}\right)/k_B T}}.$$

Taking $R_i = 3$nm, $R_c = 4.5$nm and $\kappa = 16 k_b T$, the numerical computation of the barriers from the surface and bending energy shows that the energy barrier at the vesicle edge is always smaller than the barrier corresponding to the tube, at least for the values of tension used in the experiment, as shown in Figure 2C. For tensions used in experiments from $\sigma \simeq 1\times10^{-4}$ N.m^{-1} to $\sigma \simeq 5\times10^{-4}$N.m^{-1}, the difference in energy barriers $\Delta E_{res}^{tube} - \Delta E_{res}^{ves}$ is in the range [1, 3] × $k_b T$, which in turn gives probabilities of fission in the vesicle $P_{ves} = [0.75, 0.93]$ in accordance with 75% of the breaks occurring in the vesicle observed in experiment (see Figure 1D).

Effect of GTP Concentration

The presence of GTP in the system, which entails dynamin contraction, is equivalent, at least for small deformations of the helix, to applying a homogeneous constriction force or pressure and a torque to the membrane in the dynamin domain proportional to $\Delta\mu$, the GTP hydrolysis chemical potential difference (Lenz et al., 2008). In our model, that would mean that a constant force is applied to the radius variable, which can be seen as a tilt in the energy landscape proportional to $\Delta\mu$. Thus, the total energy barrier decreases in an amount proportional to $\Delta\mu$ with a constant d that is related to the position of the intermediate state in the reaction path:

$$\Delta E_{res} = \Delta E_{tot} - d\Delta\mu = \Delta E_{tot} - c\Gamma\theta,$$

where we used the proportionality between $\Delta\mu$ and dynamin induced torque upon hydrolysis Γ, which is derived assuming the energy for constriction is coming from GTP hydrolysis and thus work done by dynamin should be $\Gamma\theta = \xi\Delta\mu$ where $\Delta\mu$ is the variation of chemical potential in the hydrolysis and ξ can be thought of as an efficiency of dynamin in the sense of how much energy is converted into work.

This gives for fission time

$$\langle t_f \rangle = \tau e^{\frac{\Delta E_{tot}}{k_b T} - c\frac{\Gamma\theta}{k_b T}}.$$

Finally, assuming an ideal dynamin solution, $\Delta\mu = k_b T\, log[GTP]$ and therefore

$$\langle t_f \rangle = \tau e^{\frac{\Delta E_{tot}}{k_b T} - c\xi\, log[GTP]}.$$

Experiments indeed show the expected dependence: $log\langle t_f \rangle = constant - c\xi\, \log[GTP]$ as shown in Figure 4F of the main text.

Torque and Final Helix Radius

As the dynamin helix hydrolyses GTP, it exerts a torque which tends to constrict the underlying membrane tubule. This torque is counteracted by the elasticity of the membrane, which favors a widening of the tubule. Here we derive a mathematical expression for the membrane's radius resulting from the balance of these two effects. We consider a cylindrical membrane constrained by a dynamin helix and first consider the geometrical relationships between the helix' radius, pitch and length. We then use them to analyze the competition between dynamin torque and membrane elasticity.

We approximate the dynamin helix by an inextensible ribbon wound around a cylinder of radius r and length L. No polymerization or depolymerization is assumed to take place over the time scales considered and the ribbon has an approximately constant width. Therefore, the total surface area of the ribbon is conserved:

$$2\pi r L = 2\pi R_u L_u,$$

where the index u refers to the initial state of the helix, prior to the introduction of GTP, when the dynamin helix is unconstricted. We define Θ as the total winding angle of the ribbon, expressed in radian. For instance, a helix that winds three times around the cylinder has $\Theta = 3\times(2\pi)$. Denoting by h the helix' pitch, this angle is given by

$$\frac{\Theta}{2\pi} = \frac{L}{h}$$

expressing the fact that adding one turn to the helix increases its length by h. To the level of approximation used here, we can assume that the pitch of the helix is constant and equal to 10nm.

We denote by κ the bending modulus of the membrane and assume that the tubule is in contact with a membrane reservoir of tension σ. Due to the small radius of the tubule (much smaller than the bare membrane equilibrium radius $\sqrt{\kappa/2\sigma}$), the energetic contribution of surface tension is small compared to the bending energy, and is neglected in the following.

The bending energy of the membrane is given by the Canham-Helfrich energy presented in the main text. Its bending term is reproduced here for convenience:

$$E_{bending} = \frac{\kappa}{2}\int_A c^2 dA.$$

For a cylindrical geometry, the curvature of the tube is $c = 1/r$ and the integral runs over a surface $A = 2\pi rL$. The bending energy thus reads $\pi\kappa L/r$, which is minimal for a flat membrane $(r \to +\infty)$. In the absence of GTP hydrolysis, the membrane is confined to a finite radius R_u by the rigidity of the dynamin helix. We represent this passive effect by an elastic equilibrium torque Γ_u implying a contribution $-\Gamma_u\Theta$ to the energy of the system.

For the purpose of determining the membrane shape, the internal, active torque induced by the dynamin polymer upon GTP hydrolysis is equivalent to an additional external torque Γ imposed on the passive helix. Therefore, dynamin activity can be described as a further lowering of the energy of the system by an amount equal to the work $\Gamma\Theta$ of this torque. Summing all the contributions to the energy, we find

$$E = -(\Gamma_u + \Gamma)\Theta + \pi\kappa\frac{L}{r} = -(\Gamma_u + \Gamma)\frac{L_u R_u}{hr} + \pi\kappa\frac{L_u R_u}{r^2}.$$

Minimizing E with respect to r, we find that

$$r = \frac{2\pi\kappa h}{\Gamma_u + \Gamma}.$$

While the passive torque Γ_u has been left unspecified until this point, it must satisfy the condition that r goes to R_u as goes to zero. This implies that $\Gamma_u = 2\pi\kappa h/R_u$, and therefore

$$r = \frac{R_u}{1 + \frac{\Gamma R_u}{2\pi\kappa h}}.$$

Using $\kappa = 20\ \mathrm{kbT} = 8 \times 10 - 20$ J, we can thus compute the torque required to obtain a constricted radius r = R_c = 5 nm to be $\Gamma \simeq 500$ pN.nm. This value is compatible with the experimental measurements presented in the main text (see Figure 4), thus validating our assessment of the role of the competition between dynamin torque and membrane bending rigidity.

SUPPLEMENTAL REFERENCES

Derényi, I., Jülicher, F., and Prost, J. (2002). Formation and interaction of membrane tubes. Phys. Rev. Lett. *88*, 238101.

Neuman, K.C., and Block, S.M. (2004). Optical trapping. Rev. Sci. Instrum. *75*, 2787–2809.

Stowell, M.H., Marks, B., Wigge, P., and McMahon, H.T. (1999). Nucleotide-dependent conformational changes in dynamin: evidence for a mechanochemical molecular spring. Nat. Cell Biol. *1*, 27–32.

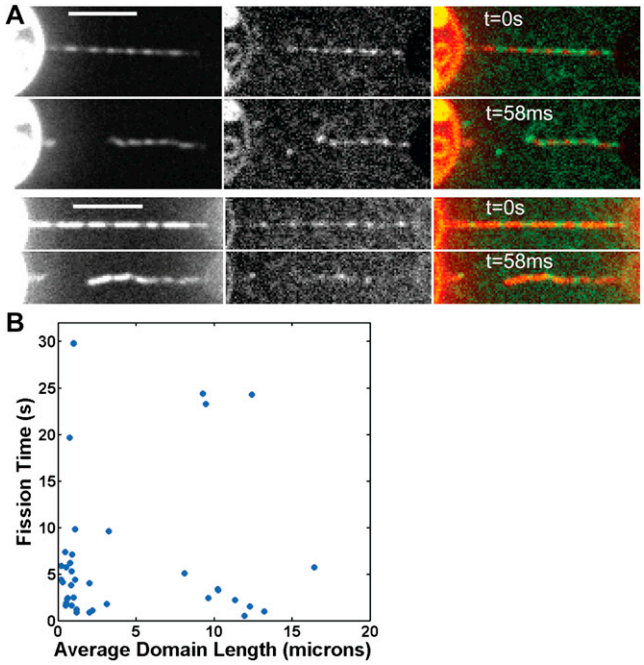

Figure S1. Fission Occurs at the Edge of Dynamin Coat and Fission Time Does Not Depend on the Polymer Length, Related to Figure 1

(A) Other examples of fission at the edge of dynamin-coated tubes equivalent to Figure 1C. Green is dynamin (center column). Red is membrane (left column). Bars are 5 μm.

(B) Fission times depending on dynamin domain length. For each experiment, dynamin was injected alone on the tube to generate separated domains. Size of the domains was controlled by controlling polymerization time through injection time. Once polymerization done, GTP was injected, and in this case, fission time was defined as time between GTP injection and break. For each data point, domain size is the average size of domains for one tube.

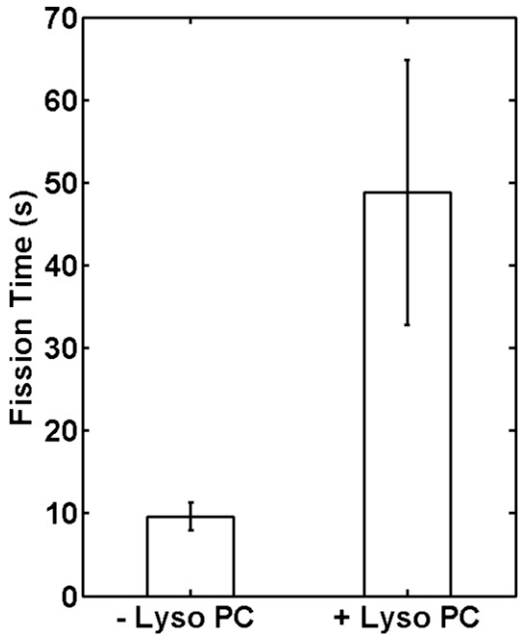

Figure S2. Fission Is Delayed by Lysolipids, in Agreement with the Hypothesis of a Hemifission Intermediate, Related to Figure 2

Histogram of average fission times for two lipid compositions: 80% EPC + 19%PIP_2 + 1%RedPIP_2 (-Lyso PC) and 50% EPC + 30% Lyso PC + 19%PIP_2 + 1% RedPIP_2 (+Lyso PC). Error bars represent SEM. The same concentrations of dynamin (2.5 μM) and GTP (150 μM) were used for both experiments. For -Lyso PC, the average fission time is $\langle t_f \rangle$ = 9.6 ± 1.7 s, N = 44. For +Lyso PC, $\langle t_f \rangle$ = 48.8 ± 16 s, N = 31. In this second case, three tubes where fission was not observed within 5 min after dynamin polymerization were taken into account, 300 s was used as an underestimate of their fission time.

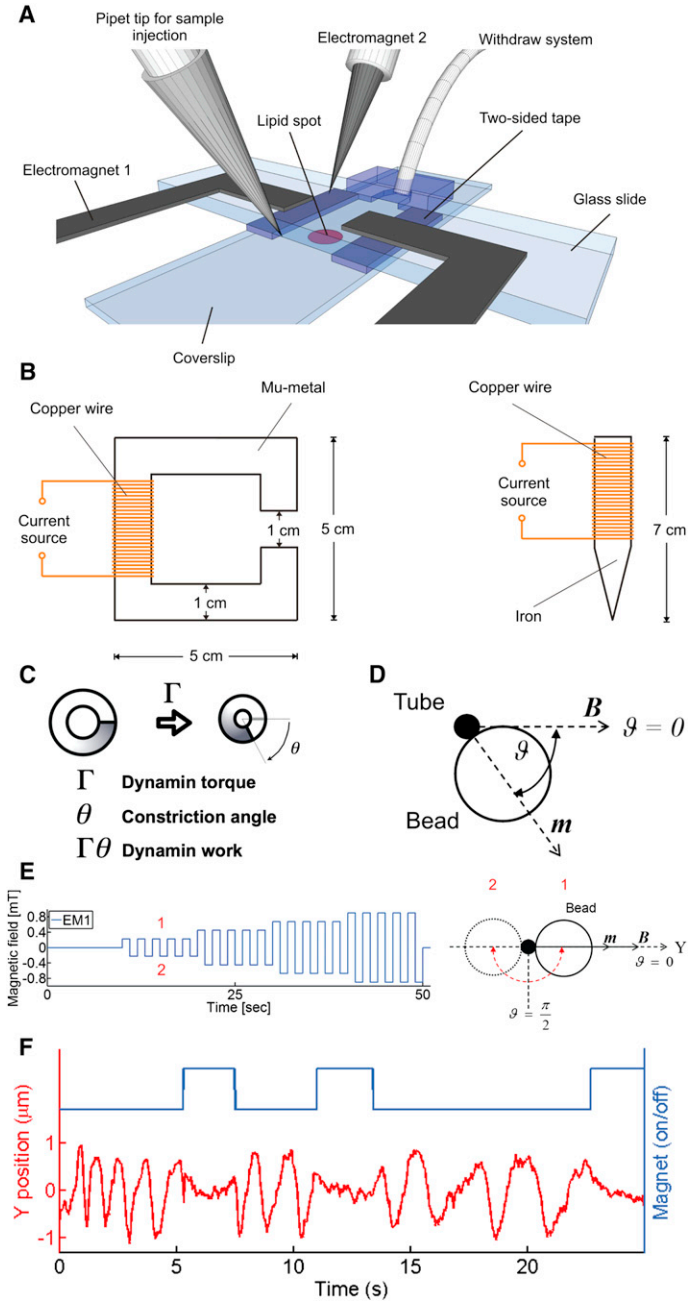

Figure S3. Dynamin Torque Counteracted by an External Torque Generated by a Magnetic Field, Related to Figure 4

(A) Schematic view of the observation chamber made of a coverslip, a glass slide and two-sided tape as a spacer. Lipids are spotted on the coverslip. The fluids are placed on one side with a pipette and withdrawn using a syringe pump from the other side of the chamber. The observation chamber is surrounded by two electromagnets EM 1 and EM 2 (dark gray) to impose a controlled magnetic field.

(B) Left: EM 1 is about 1 mm thick and consists of a coil of insulated copper wire wrapped around a mu-metal core. Right: EM 2 consists of a coil of insulated copper wire wrapped around an iron tube (1 cm diameter) with a tip to focus the magnetic field.

(C) Sketch representing dynamin torque and constriction angle.

(D) Sketch of the magnetic bead bound to the tube.

(E) Right: a schematic view of the magnetic bead bound to the membrane tube (in black). When the magnets polarity is switched, the bead passes from one side of the tube to the other. The maximum angular speed of the bead is proportional to the maximum value of the applied torque. Left: typical magnetic field profile used for torque calibration.

(F) Y-position trace (red curve) of a magnetic bead attached to a dynamin-coated tube (see Movie S5) upon GTP hydrolysis manipulated with magnetic tweezers illustrated by the blue rectangular function where the lower line marks the state of zero field ("off") and the upper line the state of an applied constant field of 4 mT ("on").

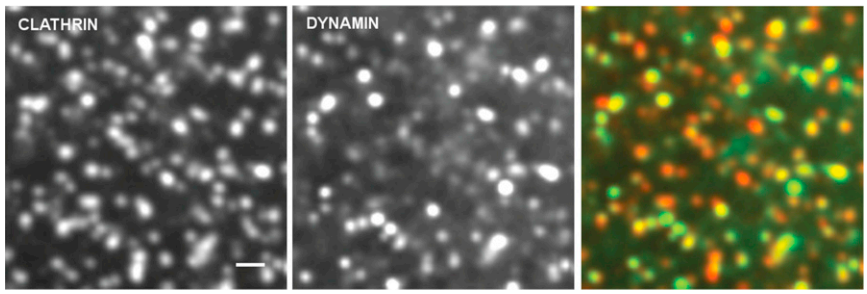

Figure S4. Dynamin and Clathrin Colocalize in Live Cells, Related to Figure 5
Colocalization of clathrin-RFP and dynamin-GFP in genome edited SKML-2 cells. Scale bar, 1 μm.

Type of file: table
Label: Table1
Filename: Morlot-SuppTable.pdf

Table S1. Fission Times Follow an Exponential Distribution, Related to Figure 3

GTP Concentration (μM)	Average Fission Time (s)	Fitted Time Parameter τ (s)
10000	6.2±0.8	6.22 (3.78, 8.65)
500	9.8±1.1	9.56 (8.50, 10.62)
100	14.2±1.7	19.62 (14.87, 24.37)
50	18.7±0.3	27.73 (25.47, 30)
10	44.8±20.8	31.47 (22.66, 40.29)
5	52.6±17.4	48.41 (41.72, 55.1)
1	85.3±8.7	89.75 (60.45, 119.2)

Fission times were measured for several tubes at different concentrations of GTP. The average fission time (center column, mean+SEM) is similar to the parameter τ given by an exponential fit of the fission time distribution (right column, fitted parameter and 95% confidence interval), which is characteristic of an exponential distribution (see also Figure 3B).

Table S2. Cholesterol and Sphingomyelin Rigidify Membranes, Related to Figure 3

Lipid Composition	Bending Rigidity (k_BT)
80% EggPC + 20% PI(4,5)P_2	16.2 ± 1.2
70% EggPC + 10%BSM + 20 %PI(4,5)P_2, 40% Cholesterol	23.5 ± 3.7
80% EggPC + 20% PI(4,5)P_2, 50% Cholesterol	25 ± 2.4
80% BSM + 20% PI(4,5)P_2, 50% Cholesterol	40.2 ± 5.4

Average bending rigidity and SEM for different lipid compositions. The bending rigidity of a GUV was calculated from the relationship between force and tension. The proportions of PIP_2 is the same for all compositions. These four lipid compositions were used to test the dependence of fission time on bending rigidity (see Figure3C).